http://dx.doi.org/10.5012/bkcs.2012.33.6.1962

Tailoring Porosity of Colloidal Boehmite Sol by Controlling Crystallite Size

Myung-Chul Park, Sung-Reol Lee, Hark Kim, In Park, and Jin-Ho Choy*

*Center for Intelligent NanoBio Materials (CINBM), Department of Chemistry and Nano Science and Department of Bioinspired Science, Ewha Womans University, Seoul 120-750, Korea. *E-mail: jhchoy@ewha.ac.kr*
Received February 24, 2012, Accepted March 16, 2012

Boehmite sols have been prepared by crystallization of amorphous aluminum hydroxide gel obtained by hydrolysis and peptization of aluminum using acetic acid. The size of the boehmite crystallites could be controlled by Al molar concentration in amorphous gel by means of controlling grain growth at nucleation stage. The size of boehmite increases as a function of Al molar concentration. With increasing boehmite crystallite size, the $d_{(020)}$ spacing and the specific surface area decreases, whereas the pore volume increases along with pore size. Especially, the pore size of the boehmite sol particles is comparable to the crystallite size along the b axis, suggesting that the fibril thickness along the b axis among the crystallite dimensions of the boehmite contributes to the pore size. Therefore, the physical properties of boehmite sols can be determined by the crystallite size controlled as a function of initial Al concentration.

Key Words : Boehmite, Porosity, Nanoparticle

Introduction

Boehmite (AlOOH) sol particles as a precursor of transitional aluminum oxide (γ-Al_2O_3) have been considerably applied for the potential porous materials such as adsorbents, catalysts and catalyst supports in many chemical process.[1-6] For the industrial applications, the fabrication of porous inorganic membrane has been extensively studied for gas separation, high temperature porous membrane reactors, and liquid separation processes.[7,8] The growing interests in these fields have resulted in the need for a very precise control of porosity such as specific surface area, pore volume, and pore size distribution.

The various synthetic procedures have been suggested in the literature in order to control particle size and morphology as well as porosity of boehmite, since the various physical properties of the boehmite depends on the crystallite size.[9-18] In general, the bottom-up approach has been performed from amorphous aluminum gels into boehmite crystallites. The crystallization of the boehmite crystallites were controlled by the synthetic conditions such as solution pH, temperature and aging time. Aluminum hydroxide gels have traditionally been prepared by the neutralization of a concentrated aluminum salt solution followed by hydrothermal treatment under basic conditions, leading to the formation of boehmite crystallites with dimensions in the micrometer range.[9,10] However, the strong interactions of the freshly precipitated alumina gels with ions from the precursor solutions can make it difficult to prepare stable colloidal solution in pure form.[18-20] To avoid this complication, alumina gel should be obtained from the hydrolysis of aluminum alkoxide, and then the stable colloidal boehmitescan be prepared by crystallization and peptization process developed by Yoldas.[21] The synthetic method also allows the control of the textural and structural properties of boehmite sols in colloidal suspensions. Although the considerable efforts for the preparation of boehmite have been carried out using the sol-gel reaction, there is still a need for further studies to exert the control of physical properties of boehmite colloidal sols.[22,23] Therefore, how to manipulate the crystallite size and control the porosity is an important issue for the preparation of boehmite in a stable colloidal solution.

In this study, we have examined the preparation of boehmite sols as a function of the initial Al concentration within a sufficient crystallization time (48 h) at a temperature below 100 °C. The prepared boehmite sols are very stable colloid, and their crystallite sizes increase with the initial Al concentration. Especially, the crystallite size of boehmites has been investigated to correlate the adsorbed water in the boehmite structure and its porous properties such as specific surface area, pore volume, and pore size distribution.

Experimental

Boehmite sols were prepared on the basis of a sol-gel method.[18] First, aluminum hydroxide gels was prepared from aluminum isopropoxide in deionized water at various molar concentrations (0.1, 0.5, 1.0, 1.5, and 2.0 M), followed by the hydrolysis reaction at 50 °C. The isopropyl alcohol produced as the by-product of the hydrolysis reaction was removed by evaporation with a rotary evaporator. The as-prepared gel was then aged at 95 °C for 48 h to crystallize boehmite, and the peptization was performed with acetic acid (acid/Al molar ratio of 0.07) for 12 h above 80 °C to form a uniform stable sol. The boehmite sols are clear colloidal suspension exhibiting a weak blue color due to light scattering. And then the resulting boehmite particles were obtained without washing process by a rotary evaporator, respectively.

X-ray diffraction patterns (XRD) were obtained with a Philips PW1830 automated powder X-ray diffractometer with Cu-Kα radiation (λ = 1.5418 Å). The morphology and grain size of the boehmite particles were examined by transmittance electron microscopy (TEM) on JEM-2000EXII operating at 200 kV. Thermal gravimetric (TG) analysis of the samples was performed on a Perkin-Elmer TG-DTA system (Pyris-Diamond TG-DTA). Approximately 10 mg of boehmite powder was loaded onto a platinum pan and heated from room temperature to 1100 °C in an air condition with a temperature ramp rate of 5 °C/min. The nitrogen adsorption-desorption isotherms were measured volumetrically at the liquid temperature (77 K) with a computer-controlled measurement system. All the samples were degassed at 150 °C for 2 h under reduced atmosphere prior to adsorption measurements. Specific surface area, pore size distribution, and total pore volume of the samples was calculated by BET method, the BJH method and the maximum adsorption at a relative pressure of 0.9, respectively.

Results and Discussion

The as-prepared gels from the hydrolysis reaction of aluminum isopropoxide are actually amorphous phase which could be crystallized into boehmite upon aging above 50 °C through a dissolution-recrystallization process. In sol-gel process of metal alkoxides, not only do hydrolysis and condensation reactions occur very rapidly, but also alcohol produced by the hydrolysis reaction causes the reverse reaction such as esterification or alcoholysis, so that it is difficult to obtain uniform and fine products. Therefore, we have carried out first removal of isopropyl alcohol after the preparation of the amorphous aluminum hydroxide gel by hydrolysis reaction, followed by the crystallization of boehmite above 80 °C through aging to complete the growth of the particles. This process is very similar to the gel-sol method developed by Sugimoto, since the boehmite nanoparticles were synthesized in the form of a stable sol from a gel.[24] In the gel-sol process, the nucleation rate is generally determined by the initial concentration of some specific precursor complexes as solute species. Consequently, this factor has influence on the particle growth for controlling final particle size. To achieve a stable boehmite sol in a desired particle size range, we have examined the variation of Al concentration as a synthetic parameter to control the rate of nucleation and crystal growth.

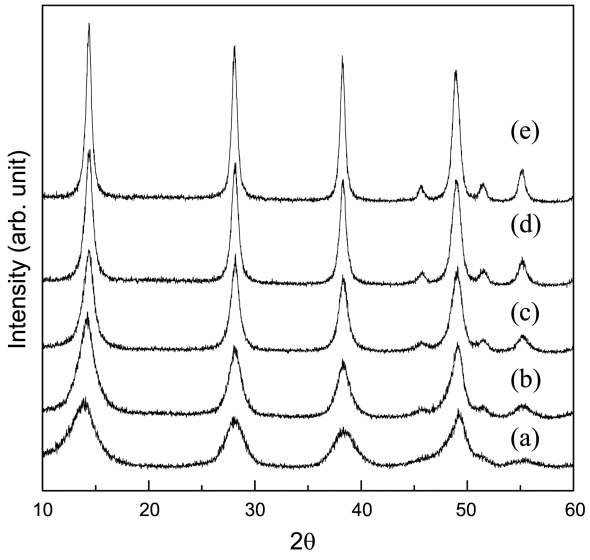

Figure 1. XRD patterns of boehmite particles prepared by crystallization at 95 °C for 48 h and the peptization reaction at 80 °C for 12 h depending on the initial Al concentration of (a) 0.1 M, (b) 0.5 M, (c) 1.0 M, (d) 1.5 M, and (e) 2.0 M.

The effect of Al molar concentration on the synthesis of boehmite sol is illustrated in Figure 1. The XRD crystallinity of the boehmite gradually increases with increasing the Al concentration. The further increase of the Al concentration could not be performed because of difficulty in handling the highly viscous suspension. However, the results evidently provide that the boehmite sol sizes are dependent on the Al concentration, indicating that the greater number of solutes enhances the grain growth of boehmite at the nucleation stage. After the re-dispersion of the as-synthesized boehmite powders in water, their suspensions are ultra-stable colloidal solutions, which are pictured in Figure 2. The colloidal solutions change from a weak blue color to a white color depending on the initial Al concentration. The solid content in colloidal suspensions could be from 20 to 30%, although the viscosity of the suspensions is observed to be different depending on the crystallite size of boehmites.[25] Thus, these results confirm that the size control of boehmite sol particles is possible by regulating the initial Al concentration in amorphous aluminum hydroxide gels.

Crystallite morphology of the boehmite particles is anisotropic, which is thin fibrils with their shortest dimension along the b axis. As seen in Figure 3, the TEM images show needle-type morphology in the longitudinal direction. Therefore, the thinnest part of the fibril crystallite can be evaluated from the broadening of the $d_{(020)}$ diffraction peak using Scherrer's formula. The XRD crystallite size, $d_{(020)}$-spacing and the other properties of the boehmite sols are summarized in Table 1. The initial Al concentration has an effect on the

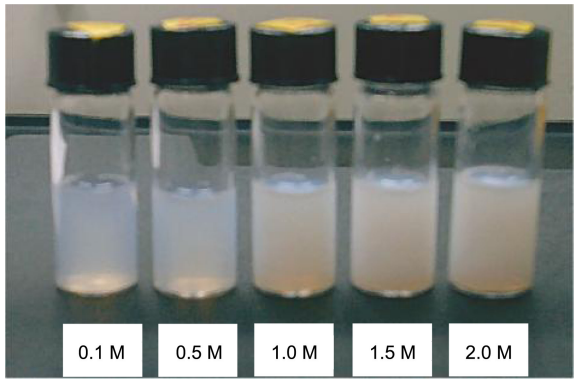

Figure 2. Photographs of boehmite sols prepared depending on the initial Al concentration (the solid content of the boehmite sol was adjusted to 5 wt %).

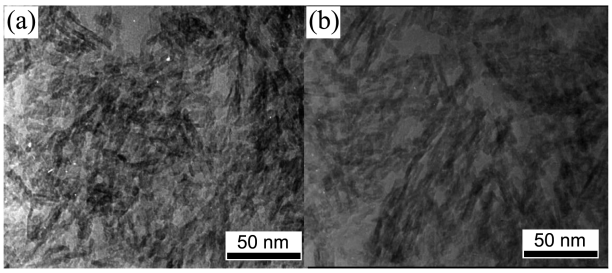

Figure 3. TEM images of the boehmite sol particles prepared with Al concentration of (a) 1 M and (b) 2 M.

structure of boehmites and thus on the final crystallite size.

The changes in the $d_{(020)}$-spacing and the crystallite size as a function of Al molar concentration are shown in Figure 4. The $d_{(020)}$-spacing of boehmite sol particles clearly decreases with increasing crystallite size. This result indicates that the change in the $d_{(020)}$-spacing is clearly related to the boehmite crystallite size in corresponding direction. Also the crystallographic results could be considered that the mole of water (x) in $AlOOH{\cdot}xH_2O$ is intercalated between boehmite octahedral double layers. The water content (x) in boehmite evaluated by a previously reported method decreases with increasing the boehmite crystallite size.[18] However, the calculated x values are too small to form a continuous water layer in the interlayer space of the boehmite and the observed shift of the $d_{(020)}$-spacing is also smaller than the theoretical thickness of a water layer (about 3 Å). Therefore, the expansion of $d_{(020)}$-spacing of boehmite with a smaller crystallite size is owing to the limited number of layer stacking as well as to excess water present mainly in the interlayers of the boehmite structure.[9]

Figure 5 shows the TG profiles of the boehmites with a different crystallite size. All samples exhibit two weight loss stages between 100 and 500 °C, which are attributed to the dehydration of water from the particles surfaces and the dehydroxylation of OH group in the phase transition from AlOOH to γ-Al_2O_3.[26,27] The first stage corresponds to the dehydration of water molecules absorbed on crystallites surface. The weight loss is comparatively low for boehmites obtained from the low Al molar concentrations, which is due

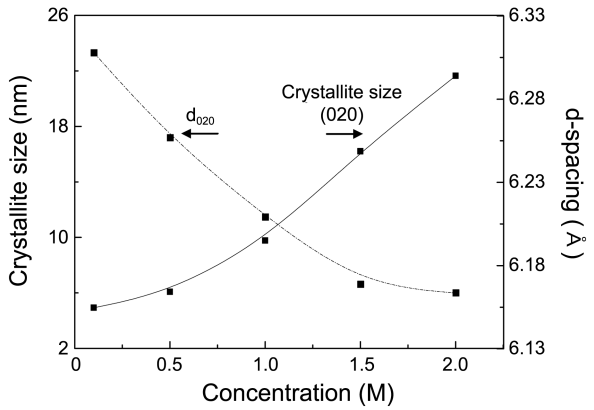

Figure 4. Plots of XRD crystallite size and $d_{(020)}$-spacing of the boehmite sol particles with respect to the initial Al concentration.

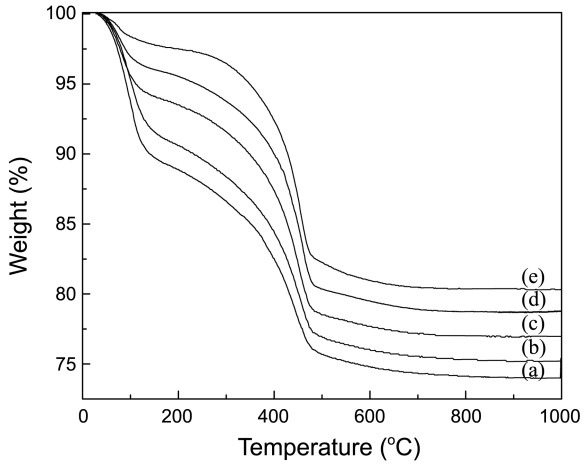

Figure 5. Thermogravimetric curves of the boehmite particles prepared with the initial Al concentration of (a) 0.1 M, (b) 0.5 M, (c) 1.0 M, (d) 1.5 M, and (e) 2.0 M.

to boehmite crystallite size and their surface areas available for water adsorption. Boehmite crystal structure has double layers of octahedra, which consist of aluminum atom coordinated by two hydroxyls and four oxygen atoms, sharing edges along the axis and vertexes along the c axis.[28,29] Therefore, the crystallite surfaces perpendicular to double layers expose oxygen atoms in low coordination. These oxygen atoms can readily react with hydroxyls and hydrogen ions, thereby allowing these surfaces to get fully covered with hydroxyls. For smaller crystallite size, the number of theses low coordination oxygen sites increases, resulting that more water molecules are adsorbed on the surface than those of larger crystallite sizes. This also suggests that boehmite sol particles with a smaller crystallite size contain a variety of excess water locally distributed in the interlayer and coordinated to hydroxyl groups on the surface.

The second weight loss stage is attributed to the dehydroxylation of OH group in the phase transition from AlOOH to γ-Al_2O_3. The boehmite with small crystallite size exhibits a gradual weight loss, whereas the boehmites with larger crystallite size show a steep weight loss around 450 °C. This is related to the hydrogen-bond strength between double layers, which is associated with the hydrogen-bond length.[26,29] This bond length decreases as boehmite crystallite size increases, indicating that the corresponding bond energy becomes stronger. Therefore, boehmites with lager crystallite size require more energy than that of the small crystallite to break the hydrogen-bond, and the different weight loss occurs depending upon the boehmite crystallite size. Consequently, the boehmites with larger crystallite size give rise to a steeper weight loss pattern during the transition to γ-Al_2O_3.

The significant changes in the texture of the boehmite sols are found in the pore properties such as specific surface area, pore size, and pore volume. Figure 6 shows N_2 adsorption-desorption isotherms of boehmite sols obtained from various Al molar concentrations. All samples exhibit the type IV adsorption isotherms indicative of mesoporous structure and

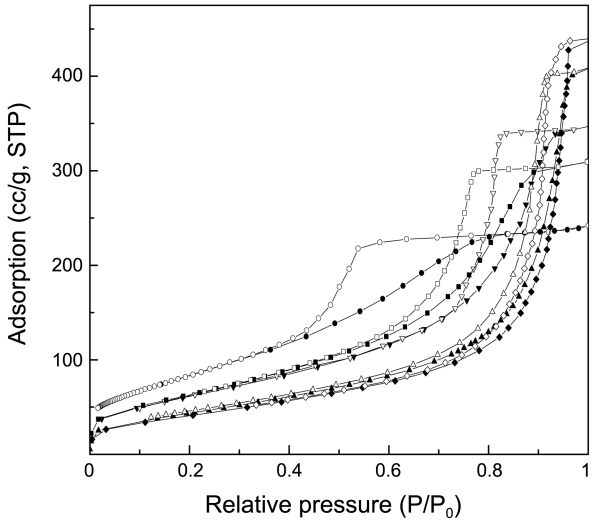

Figure 6. Nitrogen adsorption-desorption isotherms of the boehmite particles prepared withthe initial Al concentration of 0.1 M (●), 0.5 M (■), 1.0 M (▼), 1.5 M (▲), and 2.0 M (◆); filled and open marks indicate adsorption and desorption, respectively.

a H_2 hysteresis loop that closes at a relative pressure range from 0.4 to 0.8, respectively. Differences in the relative pressures are due to the modulation in pore dimensions, which is related to the increment of the pore size distributions determined from the desorption branch of isotherm using BJH method. Therefore, the porosity of boehmite sols is ultimately correlated with the crystallite size in relation to the above XRD results since boehmite particles should form the intercrystalline pore with no/little agglomeration on peptization reaction.

The change in the hysteresis loop can be observed in Figure 6, which provides pore blocking effect and pore structure rigidity generated from an assembly of coherent particles.[30,31] In the case of irregular porous materials such as boehmite particles, that is, throats in front of cavities must be filled with N_2 through the capillary condensation so that sites in unsaturated states exist with avoiding the propagation of assisted pore filling. During desorption process, filled N_2 molecules in throats act as stoppers so that a pore-blocking phenomenon takes place, which generates a sudden desorption at a capillary evaporation threshold. Especially, the plateau of the descending boundary curve for the boehmite with smaller crystallite size indicates that an appreciable pore blocking effect is present. This also suggests that the crystallite size has influenced the pore size distribution. Evidently, it is found that the pore size distribution of the boehmite sols is dependent on the crystallite size. Moreover, the pore size distributions are a little broad for the larger boehmite crystallites as shown in Figure 7, which is due to the irregular pore shape generated from the intercrystalline

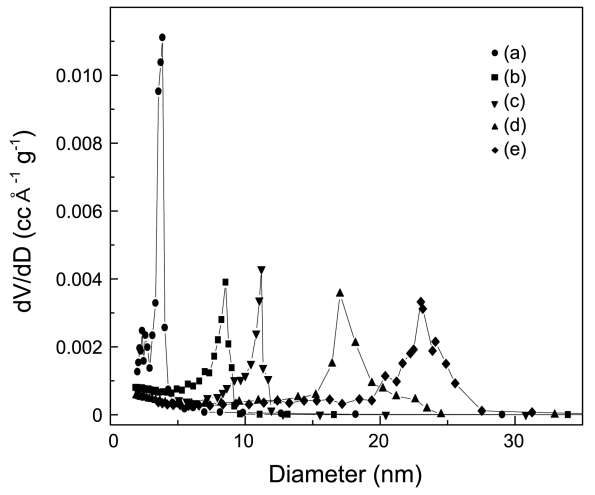

Figure 7. Pore size distribution of boehmite particles prepared with the initial Al concentration of (a) 0.1 M, (b) 0.5 M, (c) 1.0 M, (d) 1.5 M, and (e) 2.0 M.

Table 1. Summary of properties for the boehmite sols

Conc. (M)	d_{020}-spacing (Å)	Size (nm)	Surface area (m^2/g)	Pore volume (mL/g)	Pore size (nm)	xH_2O
0.1	6.31	4.9	372	0.36	38	0.83
0.5	6.26	6.7	280	0.46	85	0.73
1.0	6.22	9.7	229	0.52	112	0.55
1.5	6.18	16.4	168	0.62	170	0.40
2.0	6.16	21.6	155	0.66	230	0.24

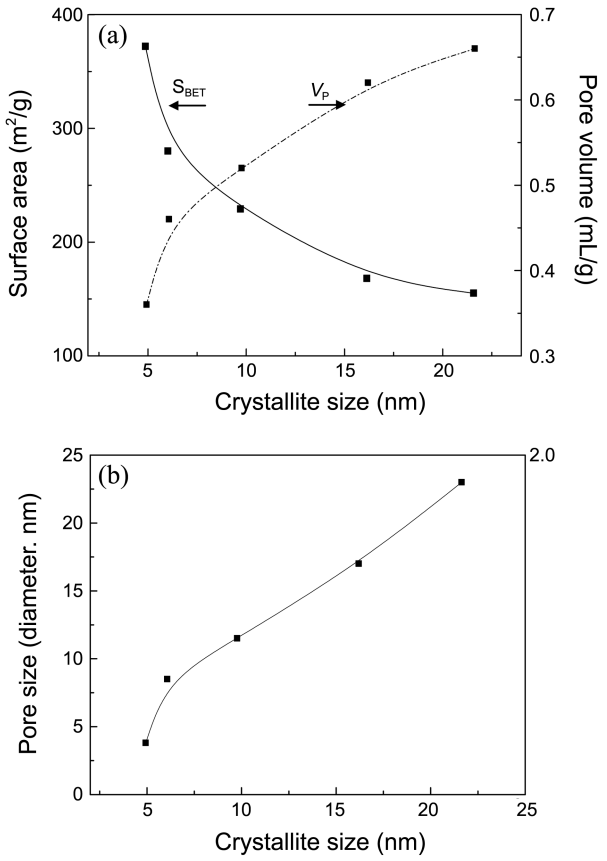

Figure 8. (a) Change in specific surface area and pore volume with respect to the crystallite size of boehmite, and (b) the relationship between the pore size and the crystallite size of boehmite sol particles.

cavities of the randomly stacked alumina nanofibrils. The initial slopping character on the descending boundary curves observed at boehmite sols with smaller crystallite size reflects the porous structure shrinkage caused by stress change of the capillary condensation during depressurization. This is attributed to swelling between the boehmite agglomerates by absorbed nitrogen, indicating that the structures in boehmite sol particles become more rigid as increasing boehmite crystallite size.

As can be seen in Table 1, it is found that the boehmite sol particles could cover the specific surface area range from 372 to 155 m^2/g, the pore volume range from 0.36 to 0.66 mL/g and the pore size range from 3.8 to 23 nm. Figure 8 shows the correlation in a specific surface area, the pore volume, and the pore size as a function of the crystallite size of boehmites. The increasing crystallite size leads to the decrease in a specific surface area, whereas the pore size of boehmite sols increases in accordance with the pore volume. One aspect to note here is that the physical properties of boehmite sols are ascribed to the crystallite size controlled as a function of Al molar concentration. Especially, the pore size is consistent with the boehmite crystallite size ($d_{(020)}$), suggesting that the fibril thickness along the b axis among the crystallite dimensions of boehmites contributes to the pore size. The effect of Al molar concentration on various porosities of boehmite sols can be also interpreted in terms of a dissolution-recrystallization mechanism which enhances the grain growth of boehmite.

Conclusion

The crystallite sizes of colloidal boehmitesol can be controlled by adjusting Al molar concentration. The increase in the initial Al molar concentration leads to the increase in crystallite size due to the enhancement of grain growth at nucleation stage. The morphology of boehmite obtained is nano-fibril and the change of the crystallite size has influence on the physical properties and the structure of boehmite. The crystallite size of the boehmite could be related to adsorbed water molecules and with the hydrogen-bond strength between octahedral double layers. The boehmites with lager crystallite size exhibit stronger interaction between double layers. Especially, the crystallite size of the boehmite shows relationships with the porosity. With increasing the crystallite size, the specific surface area decreases but the pore volume increases along with the pore size distribution. It is also found that the pore size could be affected by the b axis magnitude in boehmite crystal dimensions. From these results, the textual and structural properties of boehmite sols can be ultimately tailored by controlling crystallite size depending on the initial Al concentration.

Acknowledgments. This work was supported by RP-Grant 2010 through Ewha Womans University.

References

1. Wei, Y.; Yang, R.; Zhang, Y. X.; Wang, L.; Liu, J. H.; Huang, X. J. *Chem. Commun.* **2011**, *47*, 11062.
2. Nagai, N.; Suzuki, Y.; Sekikawa, C.; Nara, T. Y.; Hakuta, Y.; Tsunoda, T.; Mizukami, F. *J. Mater. Chem.* **2012**, *22*, 3234.
3. Liu, Q.; Wang, A.; Wang, X.; Gao, P.; Wang, X.; Zhang, T. *Microporous Mesoporous Mater.* **2008**, *11*, 323.
4. Ismagilov, Z. R.; Shkrabina, R. A.; Koryabkina, N. A. *Catal. Today* **1999**, *47*, 51.
5. Paglia, G.; Buckley, C. E.; Rohl, A. L.; Hart, R. D.; Winter, K.; Studer, A. J.; Hunter, B. A.; Hanna, J. V. *Chem. Mater.* **2004**, *16*, 220.
6. Auxilio, A. R.; Andrews, P. C.; Junk, P. C.; Spiccia, L.; Neumann, D.; Raverty, W.; Vanderhoek, N.; Pringle, J. M. *J. Mater. Chem.* **2008**, *18*, 2466.
7. Huang, X.; Meng, G.; Huang, Z.; Geng, J. *J. Membrane Sci.* **1997**, *133*, 145.
8. Oyama, S. T.; Hacarlioglu, P. *J. Membrane Sci.* **2009**, *337*, 188.
9. Okada, K.; Nagashima, T.; Kameshima, Y.; Yasumori, A.; Tsukada, T. *J. Colloid Interface Sci.* **2002**, *253*, 308.
10. Musić, S.; Dragćević, Đ.; Popović, S. *Mater. Lett.* **1999**, *40*, 269.
11. Kim, T.; Lian, J.; Ma, J.; Duan, X.; Zheng, W. *Cryst. Growth Des.* **2010**, *10*, 2928.
12. Chiche, D.; Chanéac, C.; Revela, R.; Jolivet, J. *Phys. Chem. Chem. Phys.* **2011**, *13*, 6241.
13. Buining, P. A.; Pathmamanoharan, C.; Jansen, J. B. H.; Lekkerkerker, H. N. W. J. *Am. Ceram. Soc.* **1991**, *74*, 1303.
14. Bokhimi, X.; Sánchez-Valente, J.; Pedraza, F. *J. Solid State Chem.* **2002**, *166*, 182.
15. Zhang, Z.; Hicks, R. W.; Pauly, T. R.; Pinnavaia, T. J. *J. Am. Chem. Soc.* **2002**, *124*, 1592.
16. Zhu, H. Y.; Riches, J. D.; Barry, J. C. *Chem. Mater.* **2002**, *14*, 2086.
17. Farag, H. K.; Zoubi, M. A.; Endres, F. *J. Mater. Sci.* **2009**, *44*, 122.
18. Tsukada, T.; Segawa, H.; Yasumori, A.; Okada, K. *J. Mater. Chem.* **1999**, *9*, 549.
19. Nguefack, M.; Popa, A. F.; Rossignol, S.; Kappenstein, C. *Phys. Chem. Chem. Phys.* **2003**, *5*, 4279.
20. Lee, C. M.; Sohn, Y. S. *Bull. Korean Chem. Soc.* **1985**, *6*, 329.
21. Yoldas, B. E. *Am. Ceram. Soc. Bull.* **1975**, *54*, 289.
22. Sánchez-Valente, J.; Bokhimi, X.; Hernández, F. *Langmuir* **2003**, *19*, 3583.
23. Vogelson, C. T.; Barron, A. R. *J. Non-Cryst. Solids* **2001**, *290*, 216.
24. Sugimoto, T. *Chem. Eng. Technol.* **2003**, *26*, 313.
25. Wierenga, A.; Philipse, A. P.; Lekkerkerker, H. N. W. *Langmuir* **1998**, *14*, 55.
26. Guzmán-Castillo, M. L.; Bokhimi, X.; Toledo-Antonio, A.; Salmones-Blásquez, J.; Hernández-Beltrán, F. *J. Phys. Chem. B* **2001**, *105*, 2099.
27. Krokidis, X.; Raybaud, P.; Gobichon, A. E.; Rebours, B.; Euzen, P.; Toulhoat, H. *J. Phys. Chem. B* **2001**, *105*, 5121.
28. Tettenhorst, R.; Hofmann, D. A. *Clays Clay Miner.* **1980**, *28*, 373.
29. Bokhimi, X.; Toledo-Antonio, J. A.; Guzmán-Castillo, M. L.; Mar-Mar, B.; Hernández-Beltrán, F.; Navarrete, J. *J. Solid State Chem.* **2001**, *161*, 319.
30. Gregg, S. J.; Sing, K. S. W. *Adsorption Surface Area and Porosity*, 2nd ed.; Academic Press: London, 1982.
31. Rojas, F.; Kornhauser, I.; Felipe, C.; Esparza, J. M.; Cordero, S.; Domínguez, A.; Riccardo, J. L. *Phys. Chem. Chem. Phys.* **2002**, *4*, 2346.